Daily Science Report
Stratus2007 Cruise
NOAA Ship Ronald H. Brown
C. W. Fairall (NOAA/ESRL) and R. A. Weller (WHOI)
Report #10 October 27, 2007

Summary of Recent Activities

The ship departed Panama as planned the morning of October 16. Observations were officially begun on October 18. The ship reached 20 S 75 W by the end of October 22 and spent almost two days at that location before departing to the west on October 24 and arriving at the WHOI buoy at 20 S 85 W on about 1200 GMT October 26 (Fig. 1) where we will remain for 5 days. The ESRL observations include air-sea fluxes/near-surface bulk meteorology, cloud ceilometers, radar wind profiler, scanning Doppler C-band precipitation radar, a microwave radiometer for column water vapor/liquid, and aerosols in the 0.1 to 6 micrometer range. Rawinsonde launches are being made every 4 hours (since arriving at the WHOI buoy). A sample rawinsonde profile taken at early morning local (1600 GMT) is shown in Fig. 2. A strong subsidence inversion typical of stratocumulus regions is visible at a height of about 1500 m; the relative humidity profile indicates a deep decoupled layer almost 1 km thick . Fig. 3 is a photograph taken at 1800 GMT. This photograph shows high thin clouds at the peak of afternoon warming. The cloud ceilometer cloudbase height for the last three days is shown in Fig. 4; this figure shows the change in cloud properties with the transect from 75 W to 85 W. The thicker clouds, stronger winds, and warmer water have reduced the net heat flux to the ocean to 60 W/m^2 (compared to 120 W/m^2 in the more coastal location of the DART buoy). The effect of the stratus clouds on the downward IR flux is shown in Fig. 5. Here we plot the time series of the IR flux for Oct. 27 along with an estimate of the clear sky flux (i.e./, what the flux would be if the sky were cloud free). Brief clear (ish) periods can be seen as the downward spikes in IR flux at 300.25 and 300.9. The difference between clear and overcast skies is about 70 W/m^2.

In Fig. 6 we show the data from the aerosol system for the period from October 22 through October 27. Note the lower aerosol concentrations (JD 295.5 to 296.5) which corresponded to the POC in that period. The total aerosol count decreased at the end of this period (JD 298), but notice that the larger size particles actually increased in concentration. Wind and smaller aerosols begin to decrease again at the end of the period, suggesting the approach of another POC?

One interesting issue in investigating the variability of structure and processes in the region is separating diurnal and spatial changes. One approach is to use time series at fixed points versus ship transects. Both sets of observations contain spatial (advective) and temporal changes. For example, time-height cross section is shown for the few days spent stationary at the DART buoy at 20 S 75 W (Fig. 7). The minima in air temperature and specific humidity are around 0800 local time. The transect from 75 W to 85 W is shown in near-surface flux variables (Fig.8) and sonde cross sections (Fig. 9).

Note the air temperature increases noticeably (14.5 to 17 C) and the increase is not quite matched by sea surface temperature (16 to 17 C) so the surface layer is nearly neutrally stable at the WHOI buoy. However, latent heat flux increase due to drier and windier conditions at the buoy. The sondes indicate a substantial increase in the depth of the boundary layer.

Major oceanographic activities centered on buoy operations (Fig. 10). The day was spent deploying the new Stratus mooing; the anchor went in the water at about 1700 GMT. The ship remained at the new buoy for about a day for ship-buoy intercomparisons. On October 28 we will move to the old buoy for a day of intercomparisons before extracting that system. We will be in this area for the next five days.

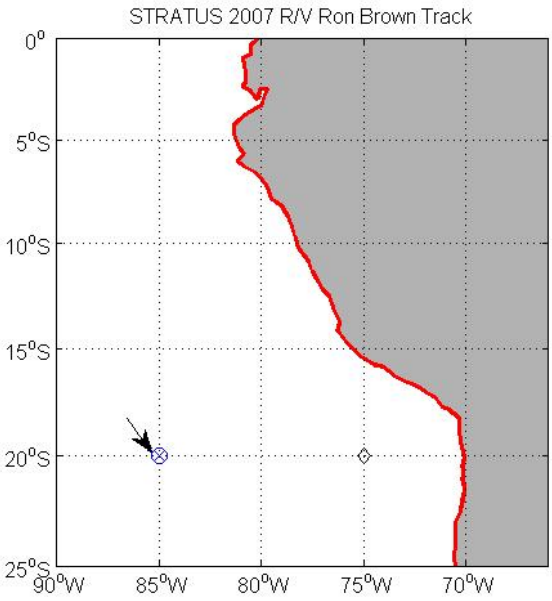

Figure 1. RHB cruise track on JD300 (Oct. 27). The diamond at 75 W is the SHOA tsunami buoy; the circle/plus at 85 W is the WHOI buoy.

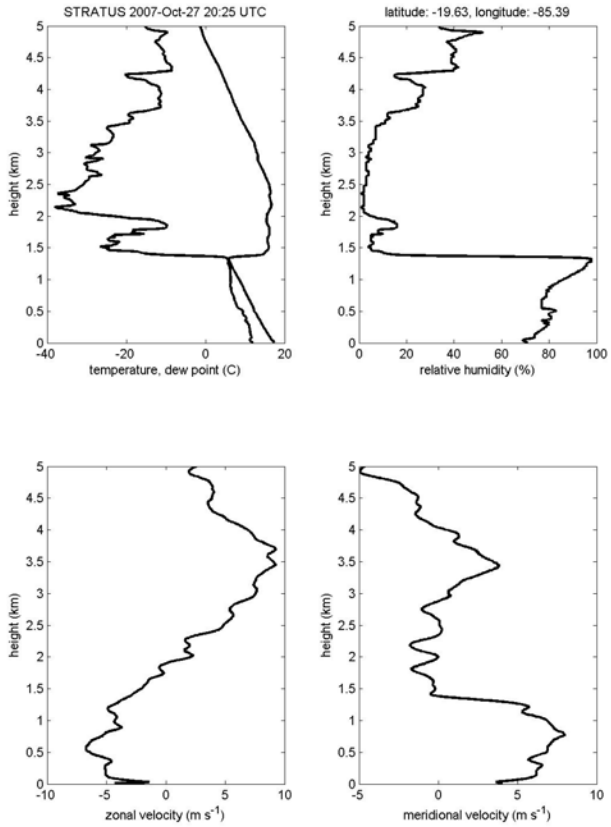

Figure 2. Rawinsonde profile 2000 GMT October 27.

Figure 3. Photograph of stratocumulus clouds 1800 GMT October 27 at 20 S 85 W.

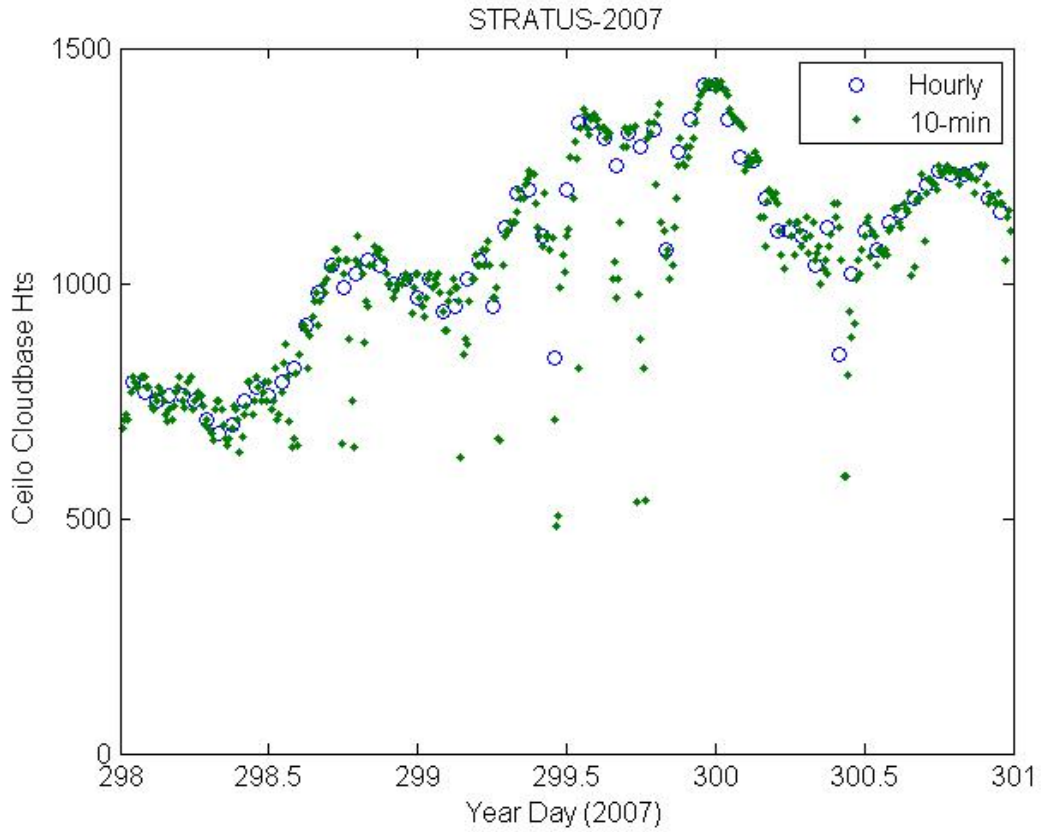

Figure 4. Time series of ceilometer cloudbase height from October 25 through October 27.

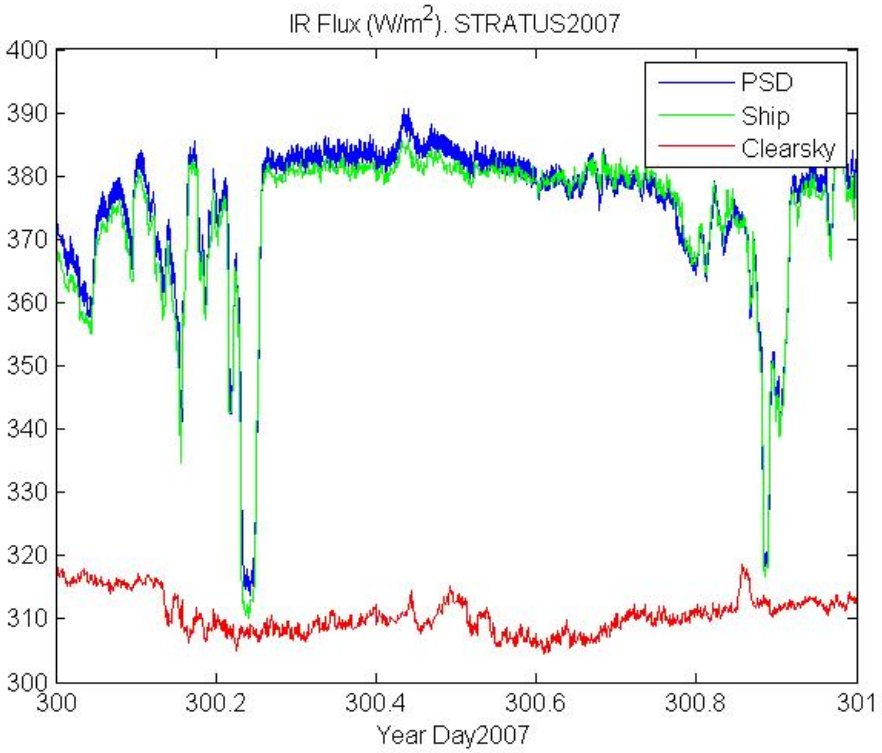

Figure 5. Time series of downward IR fluxes: measurements (blue and greenlines); model estimates of clear sky flux (red line).

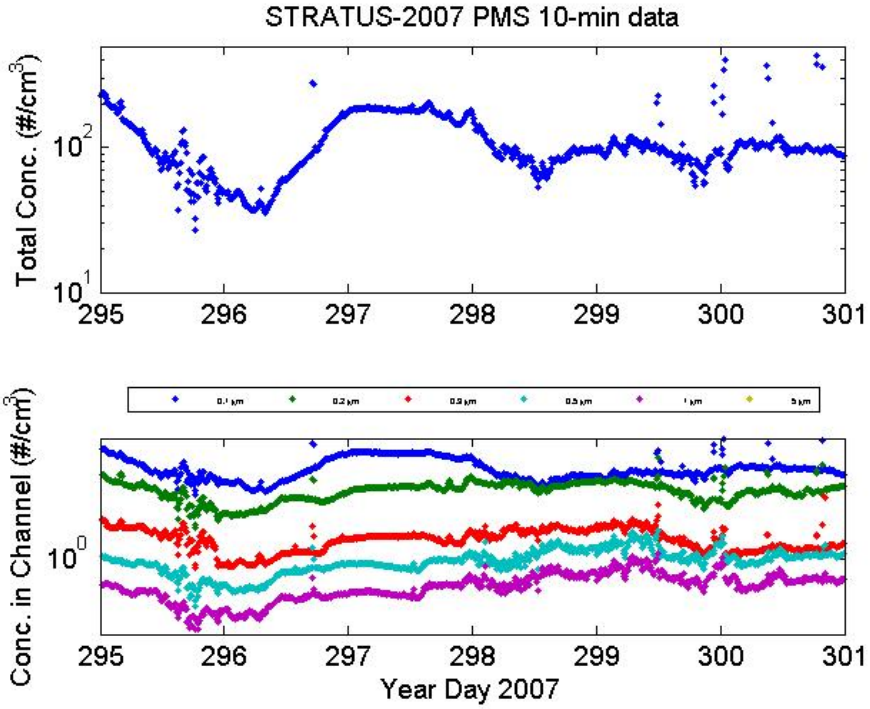

Figure 6. Time series of aerosol concentrations from October 22 through October 27. Upper panel: Total concentration for sizes from 0.1 to 5 micrometer. Lower panel: size resolved concentrations.

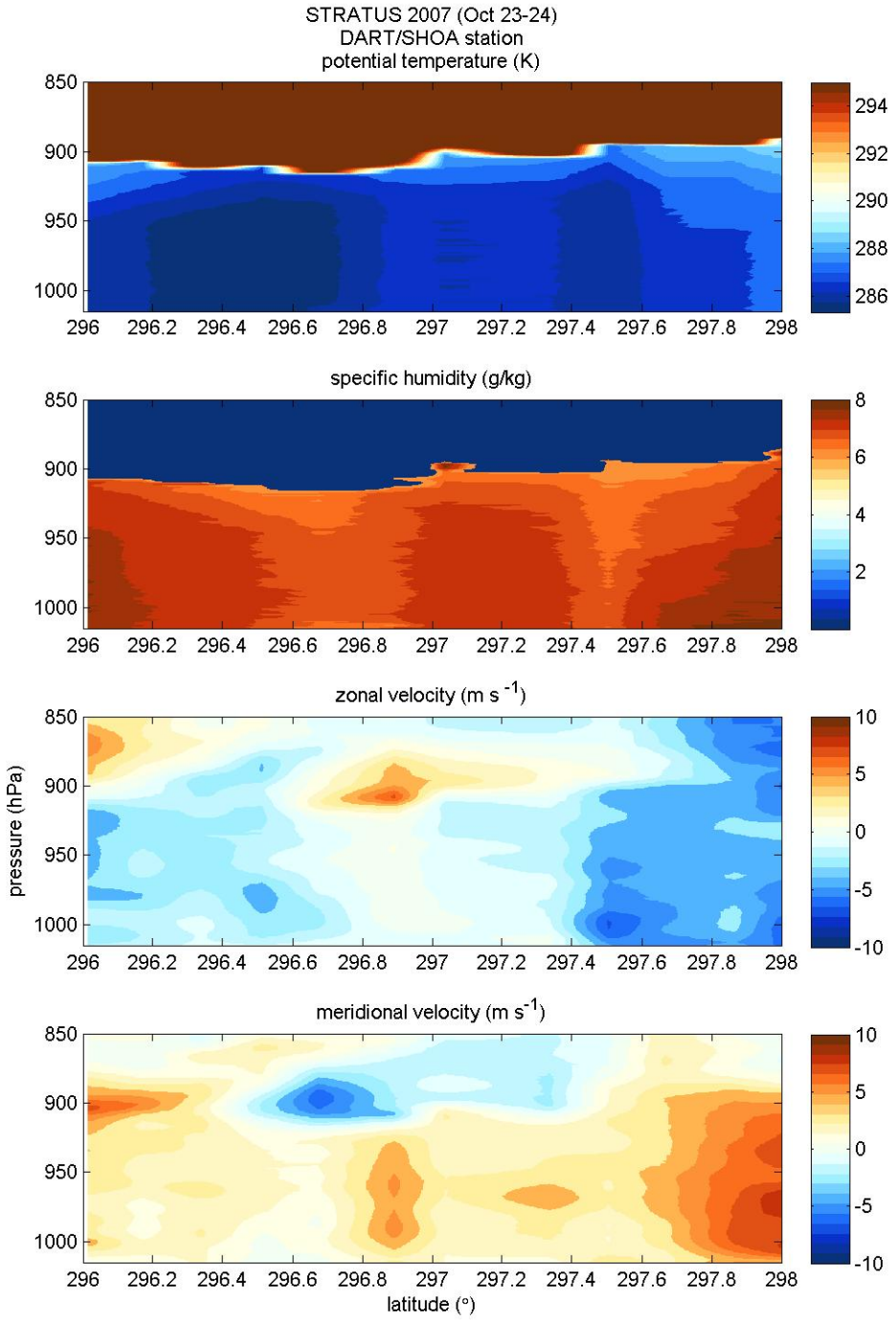

Figure 7. Time-height cross section from the rawinsonde data: top panel: temperature; second panel: relative humidity; third panel: zonal wind component; bottom panel: meridional wind component.

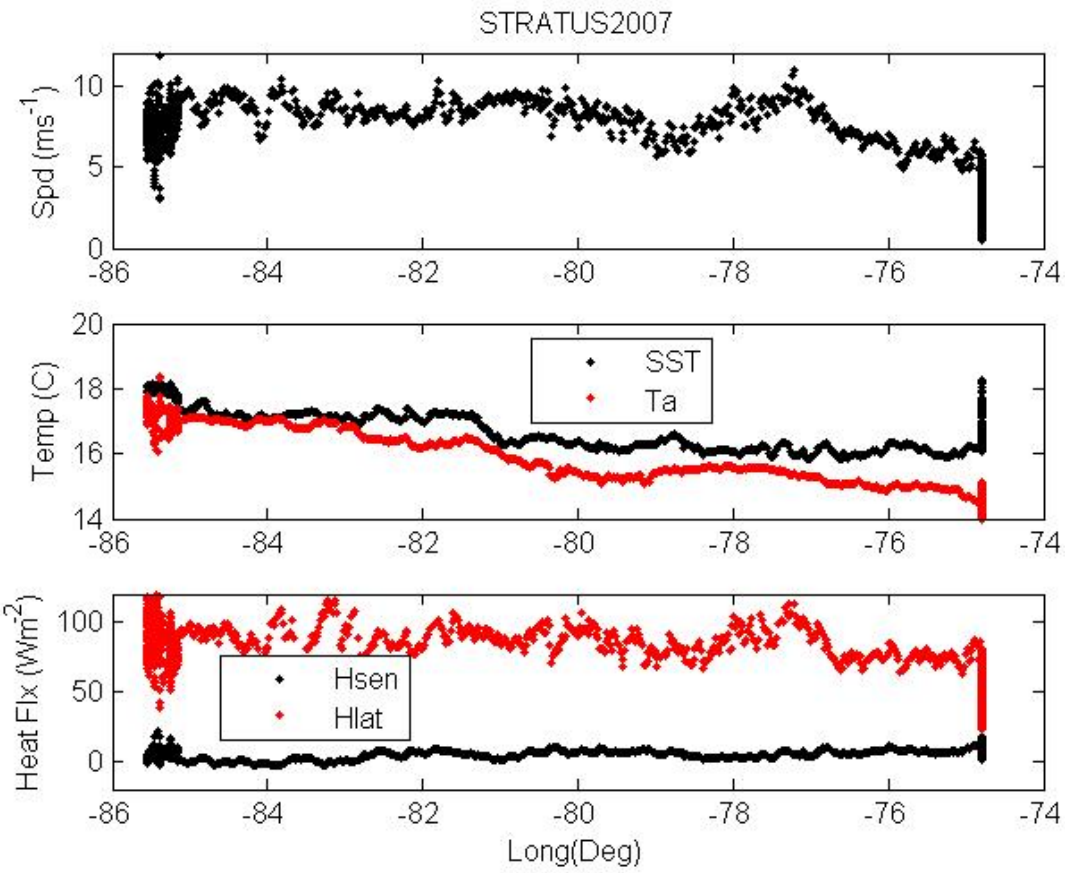

Figure 8. Longitude series from the DART buoy to the WHOI buoy: upper panel – wind speed; middle panel – SST (black dots) and air temperature (red dots); lower panel – sensible heat flux (black dots) and latent heat flux (red dots).

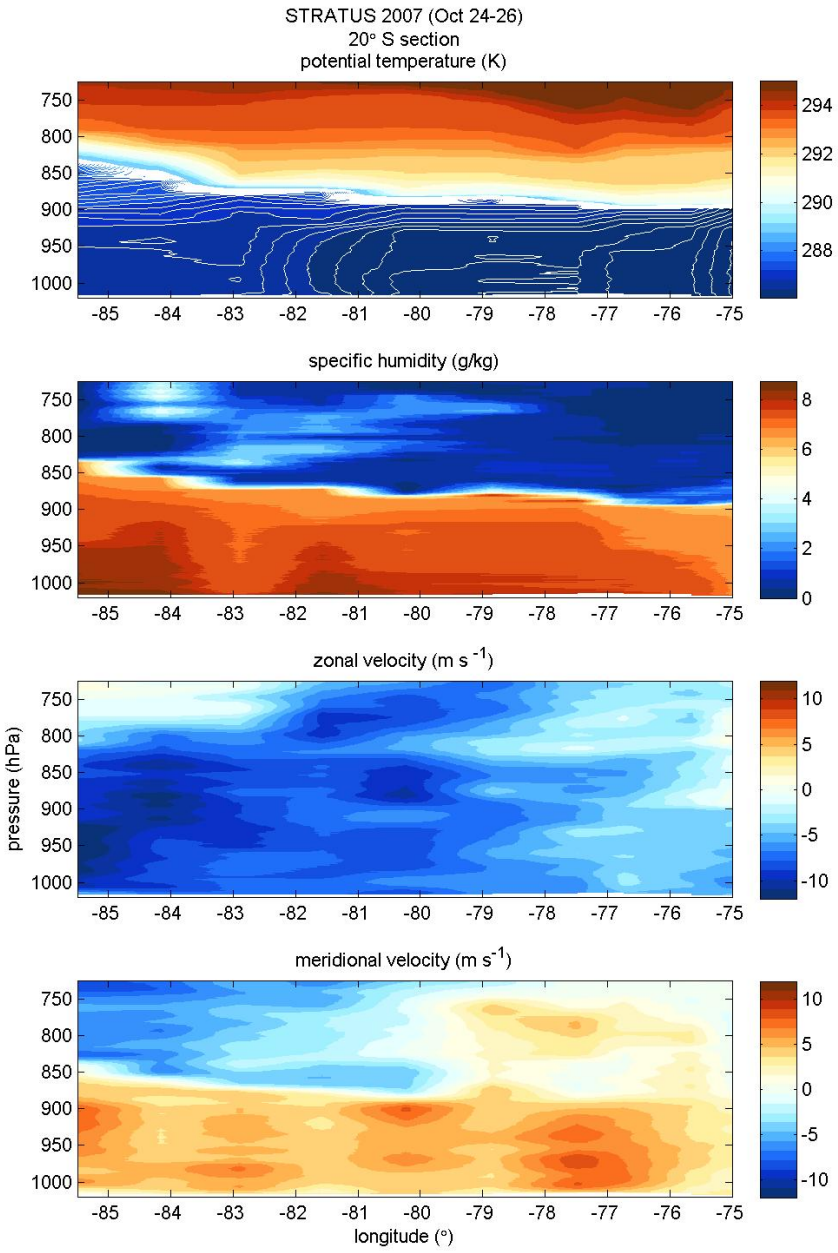

Figure 9. Longitude-height cross section from the rawinsonde data: top panel: temperature; second panel: relative humidity; third panel: zonal wind component; bottom panel: meridional wind component.

Figure 10. Photograph of WHOI buoy shortly after being placed in the water but prior to placement of subsurface sensors (aft deck of the Ronald H. Brown).